

Decoherence in a Double-Dot Aharonov-Bohm Interferometer

Björn Kubala,¹ David Roosen,² Michael Sindel,³ Walter Hofstetter,² and Florian Marquardt¹

¹*Institute for Theoretical Physics, Universität Erlangen-Nürnberg, Staudtstr. 7, 91058 Erlangen, Germany*

²*Institut für Theoretische Physik, Goethe Universität, 60438 Frankfurt/Main, Germany*

³*Physics Department, ASC and CeNs, Ludwig-Maximilians-Universität, 80333 Munich, Germany*

(Dated: November 15, 2010)

Coherence in electronic interferometers is typically believed to be restored fully in the limit of small voltages, frequencies and temperatures. However, it is crucial to check this essentially perturbative argument by nonperturbative methods. Here, we use the numerical renormalization group to study ac transport and decoherence in an experimentally realizable model interferometer, a parallel double quantum dot coupled to a phonon mode. The model allows to clearly distinguish renormalization effects from decoherence. We discuss finite frequency transport and confirm the restoration of coherence in the dc limit.

PACS numbers: 03.65.Yz, 71.38.-k, 73.63.-b, 73.63.Kv, 85.35.Ds

Introduction.- Quantum coherence and its degradation by interaction with the environment are crucial ingredients in electronic transport through nanostructures. Generically, perturbation theory suggests that coherence is fully restored in the limit of small applied bias voltage, ac frequency, and temperature. In this limit, the particles do not have enough energy to leave behind a “trace” in the environment. However, it is highly desirable to check whether such a statement remains valid beyond perturbation theory. In this work, we propose to employ the numerical renormalization group (NRG) [1] to study this question. That method can readily be applied to transport through interacting localized electronic levels, such as quantum dots and molecules. Investigating decoherence in such systems offers the advantages of (some degree of) experimental control of the type and strength of decoherence mechanisms and, on the theoretical side, of a wealth of powerful, advanced methods.

In discussing the effects of coupling a system to an environment true decoherence has to be carefully distinguished from a mere renormalization of the system’s characteristics due to the coupling. Electron-phonon (e-ph) coupling, for example, affects transport in several ways: Incoherent processes, in which phonons are absorbed or emitted, may increase or decrease the total transport through a single site [2], and coherent contributions to transport will also be renormalized. Considering an interferometer - the most obvious way to study decoherence in electronic transport - it thus turns out to be advantageous not to consider the overall change in the amplitude of the current or conductance as a measure of decoherence. Instead, we want to focus on the special case of destructive interference, i.e., the case of half a quantum of magnetic flux for an Aharonov-Bohm interferometer (ABI) (see Fig. 1). The advantage [3] is that in an interferometer with perfectly symmetric arms renormalization processes will not lift the destructive interference, and any finite current is a true sign of decoherence.

In this work, we consider a double-dot Aharonov-Bohm

interferometer (see Fig. 1), where electrons on the dots couple to a single phononic mode, representing the environment. This scenario can be experimentally realized in tunneling transport through two quantum dots placed between two electron reservoirs [4]. On the one hand, one can then consider specifically engineered phononic environments, for instance, for quantum dots defined within free standing nanobeams [5], or a quantum dot coupling to a cantilever [6]; on the other hand, the simple scenario can easily be generalized to model multiple phonon modes in standard heterostructures or molecular electronics [7]. We will focus on the linear ac conductance, which is readily accessible by NRG and of great current interest in general [8, 9]. The nonperturbative NRG results will be complemented by nonequilibrium Green’s functions (NEGF) [10] methods.

The Model.- Our system is described by the Hamiltonian $\hat{H} = \hat{H}_{\text{imp}} + \sum_{\alpha=L/R} (\hat{H}_{\text{res},\alpha} + \hat{H}_{T,\alpha})$ with lead Hamiltonian $\hat{H}_{\text{res},\alpha} = \sum_k \epsilon_{k\alpha} \hat{c}_{k\alpha}^\dagger \hat{c}_{k\alpha}$, and spinless electrons on two degenerate dot levels, $n = 1, 2$ coupling to

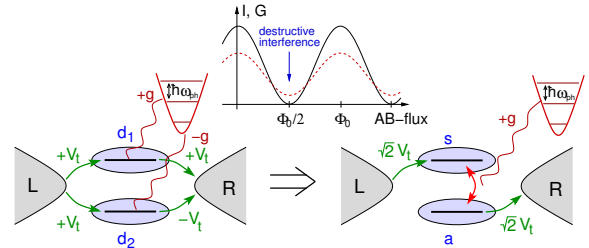


Figure 1. A double-dot Aharonov-Bohm interferometer. Decoherence suppresses the amplitude of AB oscillations (dashed line). At destructive interference, $\phi_{AB} = \Phi_0/2$, only incoherent transport processes contribute in a symmetric setup. Mapping the Hamiltonian to (anti)symmetric combinations of the dot levels allows for a transparent exploitation of this cancellation of coherent transport.

a single phonon mode,

$$\hat{H}_{\text{imp}} = \sum_{n=1,2} \varepsilon \hat{d}_n^\dagger \hat{d}_n + \hbar \omega_{\text{ph}} \hat{b}^\dagger \hat{b} + g(\hat{b} + \hat{b}^\dagger)(\hat{d}_1^\dagger \hat{d}_1 - \hat{d}_2^\dagger \hat{d}_2), \quad (1)$$

where the level energy, ε , is taken with respect to the Fermi level of the leads. Assuming an electron-phonon coupling of equal magnitude, but different signs for the two dots, the phonons effectively act as a kind of 'which-path' detector decohering the electrons.

In a symmetric, destructive interferometer, i.e. for a tunneling Hamiltonian, $\hat{H}_{T,\alpha} = \sum_{k,n=1,2} V_{\alpha,n} \hat{c}_{k\alpha}^\dagger \hat{d}_n + c.c.$, where $V_{L/R,1} = V_{L,2} = -V_{R,2} = V_t$ it is decoherence alone, which allows for transport, overcoming the destructive interference. This is seen by mapping the Hamiltonian to a new basis, $\hat{a}/\hat{s} = (\hat{d}_1 \mp \hat{d}_2)/\sqrt{2}$, of (anti)symmetric combinations of the original dot levels. The impurity Hamiltonian then reads

$$\hat{H}_{\text{imp}} = \varepsilon(\hat{s}^\dagger \hat{s} + \hat{a}^\dagger \hat{a}) + g(\hat{b} + \hat{b}^\dagger)(\hat{s}^\dagger \hat{a} + \hat{a}^\dagger \hat{s}) \quad (2)$$

with the (anti)symmetric level coupling to the left (right) lead only with tunneling matrix elements $V_{L,s} = V_{R,a} = \sqrt{2}V_t$ and $V_{R,s} = V_{L,a} = 0$, see Fig. 1. It decouples into separated left and right parts for $g = 0$, whereas transport across the interferometer becomes possible due to a tunneling term between the two new levels, which is coupled to the phonon mode. While it is obvious that the noninteracting contribution vanishes, we will later show that destructive interference also cancels renormalized processes, reflected in the vanishing of certain classes of diagrams after performing the mapping. This particularly advantageous feature of only observing (in calculation and experiment) incoherent transport processes offered by the setup considered here was not present in other theoretical studies of various interference effects in related setups [11] nor in studies of e-ph interaction for a single dot [12–15].

Techniques.- We will present two approaches to study this system. *First*, we employ non-equilibrium Green's function (NEGF) theory, where, based on the exact non-interacting result [16], electron-phonon interaction is perturbatively included using Keldysh diagrams. Particularly tailored to treat nonequilibrium situations, which can easily be realized in quantum dot systems by an applied dc bias, the NEGF or Keldysh method [10] has been widely used as a physically transparent tool to investigate e-ph interaction in such systems, often, as here, in a perturbative manner [12–14] or employing extensions of the polaron approach [13, 15], which allows tackling strong electron-phonon coupling for weakly tunnel-coupled systems. In this work, we focus on the *linear ac-conductance* $\mathcal{G}_{\alpha\beta}$, giving the finite frequency current $I_\alpha(\omega_{\text{ac}}) = \mathcal{G}_{\alpha\beta}(\omega_{\text{ac}}) V_\beta(\omega_{\text{ac}})$ flowing out of lead α as response to a small ac-excitation voltage V_β of frequency ω_{ac} applied to lead β [17]. It is connected to a (retarded) current-current correlator, $\mathcal{G}_{\alpha\beta}(\omega_{\text{ac}}) =$

$[K_{\alpha\beta}(\omega_{\text{ac}}) - K_{\alpha\beta}(0)]/(i\omega_{\text{ac}})$, where

$$K_{\alpha\beta}(\omega_{\text{ac}}) = -\frac{i}{\hbar} \int_0^\infty dt e^{i\omega_{\text{ac}}t} \langle [\hat{I}_\alpha(t), \hat{I}_\beta(0)] \rangle. \quad (3)$$

To calculate this correlator, and, hence, the ac conductance, we use a recently developed Meir-Wingreen-type formula for the linear ac conductance [18], which allows straightforward diagrammatic calculations perturbatively including electron-phonon interaction - complementing previous works building on a fully time-dependent Green's function formalism [19] (see e.g., [20], treating electron-electron interactions) and rate-equation approaches [21].

While the perturbative NEGF-approach is only valid for weak electron-phonon interaction, our *second* approach, the numerical renormalization group method (NRG), invented by Wilson in the late 1970s [1], is especially tailored for strongly interacting systems. Throughout the last decades numerous enhancements of the numerical renormalization group method have been introduced, ever improving the accuracy of correlation functions [22–25] and opening the possibility to study quantum impurity systems coupled to a bosonic bath [26]. Here, we present to our best knowledge the first NRG calculation of ac conductance in a quantum dot system with an additional bosonic degree of freedom (cf. NRG studies on ac conductance with electron-electron interaction, for instance, in the Kondo regime [27], and investigations of electron-phonon coupling effects on linear dc-conductance, spectral density and spin and charge susceptibilities in [28, 29]). For a quantum impurity system with a fermionic bath and an additional bosonic mode coupled to the impurity directly, the numerical renormalization group can be applied in a similar fashion as in the "pure" fermionic case without the bosonic mode. The mapping to the Wilson chain is not affected by the additional bosonic mode [25, 28], since the bosons only enter in the very first step of the iterative diagonalization procedure. We implemented a NRG algorithm using the reduced density matrix [23] as well as the complete basis of the underlying Fock space. Furthermore, we performed a z -trick averaging [30] over 32 slightly different discretizations of the conduction band to improve on the logarithmic resolution of energy (and thereby also frequency) around the Fermi energy inherent to NRG. In that manner, reliable numerical results up to frequencies of some ten percent of the bandwidth could be achieved with reasonably small numerical errors and artifacts.

Results and interpretation.- To investigate the effects of *weak electron-phonon coupling* on ac-transport, we employ NEGF, considering contributions to the ac-conductance from diagrams with up to a single phonon line, which gives contributions up to order $\mathcal{O}(g^2)$. Using the mapping to (anti)symmetric dot levels in a diagrammatic representation for the ac conductance automatically exploits the main characteristic of transport in the

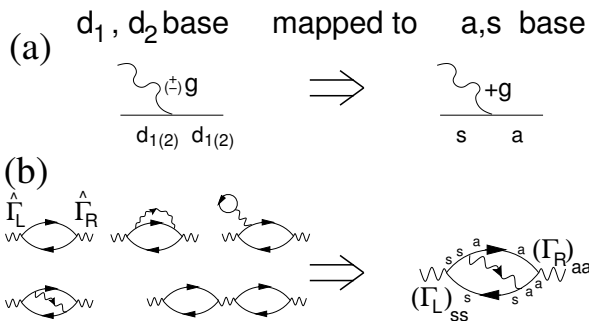


Figure 2. Mapping the Hamiltonian to (anti)symmetric combinations of the dot levels: the mapped electron-phonon interaction vertex (a) restricts the number and type of diagrams in a perturbative calculation of ac conductance (b), reflecting the destructive interference of all coherent contributions. (Solid lines denote electron Green’s functions, wiggly lines stand for phonon propagators.)

symmetric destructive ABI, namely the complete cancellation of coherent transport processes due to destructive interference. For instance, considering the ac conductance, $\mathcal{G}_{LR}(\omega_{ac})$, there are a zeroth-order and several second-order diagrams constructable from the original e-ph interaction vertex, Fig. 2, while no zeroth-order and only a single second-order diagram can be constructed from the mapped e-ph coupling vertex and the mapped lead-dot couplings. The nonexistence of those diagrams reflects the notion that in the destructive ABI the coherent zero-order contribution, as well as contributions, where transport is “merely renormalized”, will interfere destructively and thus vanish. There are, however, diagrammatic contributions for the “diagonal” conductances $\mathcal{G}_{LL/RR}(\omega_{ac})$, describing electrons tunneling back and forth between the (anti)symmetric level and the (left) right lead, as the chemical potential of the lead is varied with frequency ω_{ac} . The noninteracting result thus found (see the lower right panels of Fig. 3), which is also accessible by simpler techniques [9, 19], reproduces for small frequencies the universal behavior of a mesoscopic RC-circuit with a quantized charge relaxation resistance [8, 9]. The second-order contribution to \mathcal{G}_{LL} constitutes a small correction to the noninteracting result, which yields additional features at $\omega_{ac} = \epsilon + \omega_{ph}$. Turning to the conductance across the interferometer, \mathcal{G}_{LR} , we find, as argued above, no zeroth order, and only a single, topologically distinct diagram in second order, namely an electronic loop with a crossing phonon line [see Fig. 2(b)]. One can now easily use Keldysh diagrammatic rules to find the corresponding integral expression for the ac conductance in terms of the electronic Green’s functions and the bare phononic propagators $D_{E'}^{R/A} = (E' - \omega_{ph} \pm i\eta)^{-1} - (E' + \omega_{ph} \pm i\eta)^{-1}$. Interestingly, there are contributions from the δ -peak at the phonon energy ω_{ph} as well as from the principal-value part. For the dissipative real part of the conductance,

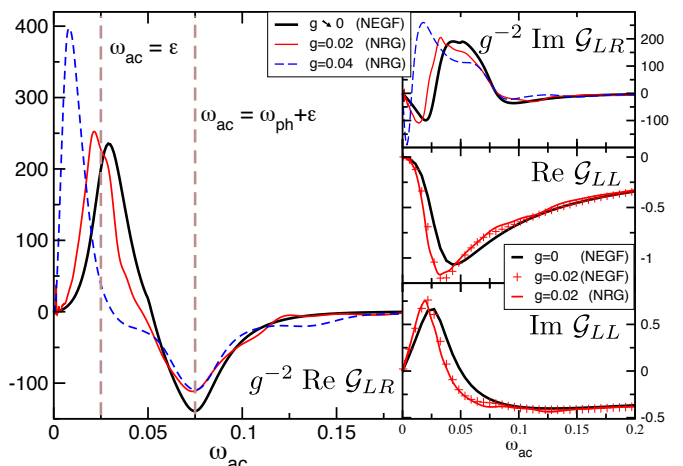


Figure 3. ac conductance through the destructive ABI. In the limit of weak electron-phonon coupling NRG and perturbative calculations match. For stronger e-ph coupling, $g/\omega_{ph} \approx 1$, additional sidepeaks at $\omega_{ac} = \epsilon + n\omega_{ph}$ ($n = 1, 2, \dots$) appear, and the first resonance is shifted to lower frequency. $\mathcal{G}_{LR}(\omega_{ac} = 0) \equiv 0$ is found also for strong e-ph coupling. Parameters are $\omega_{ph} = 0.05$, $\epsilon = 0.025$, $\Gamma = 2\pi(\rho_L + \rho_R)|V_i|^2 = 0.02$ in units of the bandwidth, conductances in units of e^2/h , and we consider the zero temperature limit and no dc-bias.

$\text{Re}\mathcal{G}_{LR}$, (see left panel of Fig. 3), we find that contributions from the latter yield a resonant peak at $\omega_{ac} = \epsilon$. Around $\omega_{ac} = \epsilon + \omega_{ph}$, where the excitation frequency is in resonance with the dot level position after the excitation of a phonon, there is a smaller negative peak, stemming from the δ -contributions. Corresponding features at the same frequencies are found for the imaginary part, $\text{Im}\mathcal{G}_{LR}$.

Investigating *strong electron-phonon coupling*, comparisons of NRG calculations to the perturbative results are shown in Fig. 3. For weak e-ph coupling, there is good qualitative and also quantitative agreement between NRG and the perturbative results: In the limit $g \searrow 0$, we reach the noninteracting results for \mathcal{G}_{LL} (thick black lines in the two lower right panels of Fig. 3), while for \mathcal{G}_{LR} we recover the perturbative, $\mathcal{O}(g^2)$, result derived above. The left panel of Fig. 3 also demonstrates the main effects of stronger e-ph coupling on $\text{Re}\mathcal{G}_{LR}$. Most importantly, one finds additional resonances at sidebands of the level energy, $\omega_{ac} = \epsilon + n\omega_{ph}$ ($n = 1, 2, \dots$), which stem from processes involving several phonons. Furthermore, we observe a shift of the first resonance from $\omega_{ac} \approx \epsilon$ to smaller frequencies reminiscent of a polaron shift.

In the following, we want to highlight two particular remarkable features of our results at low frequency. The *first*, observable already in the weak coupling limit, is the fact, that ac transport is already possible for excitation frequencies smaller than the phonon energy, $\omega_{ac} < \omega_{ph}$. Let us first emphasize, that this is in striking contrast to the case of finite-bias dc transport, where in the

weak coupling limit there is a sharp threshold for incoherent transport processes becoming possible only for $eV_{\text{dc}} \geq \omega_{\text{ph}}$. Using the mapping to (anti)symmetric dot states the dc current through a destructive ABI can be shown to contain only incoherent contributions. These contributions are characterized by explicit appearance (cf. Eq. 66 in Ref. [12]) of self-energies, $\Sigma^{\lessgtr, \text{ph}}$, due to emission or absorption of phonons. In lowest order in the e-ph coupling (and for zero temperature) transport takes place through two “transport channels” at $\omega = \epsilon$, $\epsilon + \omega_{\text{ph}}$ within a transport window, $\mu_L > \omega > \mu_R + \omega_{\text{ph}}$. In particular, the resulting I-V curve has a sharp gap at low bias, $eV_{\text{dc}} < \omega_{\text{ph}}$, as any incoherent transport process necessarily involves the emission of a phonon, whose energy has to be provided by the applied bias. The naive expectation, that in ac transport the frequency of the infinitesimal ac-excitation voltage providing energy for emission of phonons acts in a similar manner does not hold. In fact, subthreshold ac transport apparently is possible without the real emission of phonons. Considering the Hamiltonian of the destructive ABI in the mapped base, we see that virtual tunneling back and forth processes between symmetric and antisymmetric levels with emission and absorption of phonons will yield an effective charge-charge interaction between the two sites. Such interaction then leads to finite ac conductance, but vanishing dc conductance, just like the electrostatic interaction in a plate capacitance.

While both of these arguments explain the vanishing of conductance in the dc limit in lowest order in the e-ph coupling, note as a *second*, most important feature of the results in Fig. 3, that our NRG results indicate that this holds for strong coupling also. Indeed, while in a lowest-order process phonons can only be excited exactly at their bare frequency ω_{ph} , considering higher orders, one may naturally ask about the effects of the broadening of the phonon propagator due to coupling to the electrons. Some (though not all) higher-order effects can thus be captured by calculating the electronic self-energies with a phonon propagator dressed with electronic polarization bubbles. In the dc-case, one finds that electrons can indeed absorb an energy up to eV from the phononic bath broadened by coupling to the electrons, instead of needing to emit ω_{ph} as in lowest order. Nonetheless, the weight of such contributions is small leading to a current dependence $I \propto (eV)^3$ for small bias voltage for the considered higher-order contributions in the e-ph coupling and consequently a vanishing linear conductance at zero frequency. This agrees with the dc limit of our NRG results for the ac conductance, which indicates as discussed that all higher-order contributions to the linear zero-temperature conductance vanish. We thus confirm the naive perturbative argument, that there are no incoherent transport processes at vanishing frequency, temperature and transport voltage.

Conclusions.- We have studied decoherence and the effects of electron-phonon coupling on ac transport in a double-dot interferometer. A diagrammatic calculation reveals that renormalization processes can be clearly distinguished from decoherence for the case of destructive interference, and it explains low frequency transport as a consequence of phonon-mediated charge-charge interactions in a mapped system. NRG calculations for stronger coupling show characteristic features due to multi-phonon processes. With increasing coupling, the phonon mode broadens and effectively yields a continuous environment spectrum. Nevertheless, the nonperturbative NRG result confirms that coherence is fully restored in the zero-frequency limit of the linear conductance at zero temperature.

We acknowledge support by the DFG (Emmy-Noether, NIM, SFB TR 12), GIF and DIP.

-
- [1] K. G. Wilson, Rev. Mod. Phys. **47**, 773 (1975).
 - [2] O. Tal, M. Krieger, B. Leerink, and J. M. van Ruitenbeek, Phys. Rev. Lett. **100**, 196804 (2008) and Refs. within.
 - [3] F. Marquardt and C. Bruder, Phys. Rev. B **68**, 195305 (2003); J. König and Y. Gefen, Phys. Rev. Lett. **86**, 3855 (2001).
 - [4] A. W. Holleitner, C. R. Decker, H. Qin, K. Eberl, and R. H. Blick, Phys. Rev. Lett. **87**, 256802 (2001); M. Sigrist, T. Ihn, K. Ensslin, D. Loss, M. Reinwald, and W. Wegscheider, Phys. Rev. Lett. **96**, 036804 (2006).
 - [5] E. M. Weig, R. H. Blick, T. Brandes, J. Kirschbaum, W. Wegscheider, M. Bichler, and J. P. Kotthaus, Phys. Rev. Lett. **92**, 046804 (2004).
 - [6] S. D. Bennett, L. Cockins, Y. Miyahara, P. Grütter, and A. A. Clerk, Phys. Rev. Lett. **104**, 017203 (2010).
 - [7] M. Galperin, M. A. Ratner, and A. Nitzan, J. Phys. Condens. Matter **19**, 103201 (2007); R. Härtle, C. Benesch, and M. Thoss, Phys. Rev. B **77**, 205314 (2008).
 - [8] J. Gabelli, G. Feve, J. M. Berroir, B. Placais, A. Cavanna, B. Etienne, Y. Jin, and D. C. Glattli, Science **313**, 499 (2006).
 - [9] M. Büttiker, H. Thomas, and A. Prêtre, Phys. Lett. A **180**, 364 (1993).
 - [10] J. Rammer and H. Smith, Rev. Mod. Phys. **58**, 323 (1986).
 - [11] K. Haule and J. Bonča, Phys. Rev. B **59**, 13087 (1999); V. Meden and F. Marquardt, Phys. Rev. Lett. **96**, 146801 (2006); O. Hod, R. Baer, and E. Rabani, Phys. Rev. Lett. **97**, 266803 (2006); A. Ueda and M. Eto, New J. Phys. **9**, 119 (2007); W. Gong, Y. Zheng, J. Wang, and T. Lü, Phys. Status Solidi B **245**, 1175 (2008).
 - [12] P. Hyltdgaard, S. Hershfield, J. H. Davies, and J. W. Wilkins, Ann. Phys. (NY) **236**, 1 (1994).
 - [13] A. Mitra, I. Aleiner, and A. J. Millis, Phys. Rev. B **69**, 245302 (2004).
 - [14] R. Egger and A. O. Gogolin, Phys. Rev. B **77**, 113405 (2008); O. Entin-Wohlman, Y. Imry, and A. Aharony, Phys. Rev. B **80**, 035417 (2009).
 - [15] N. S. Wingreen, K. W. Jacobsen, and J. W. Wilkins, Phys. Rev. B **40**, 11834 (1989); K. Flensberg, Phys. Rev.

- B **68**, 205323 (2003); J. Koch, F. von Oppen, Y. Oreg, and E. Sela, Phys. Rev. B **70**, 195107 (2004).
- [16] B. Kubala and J. König, Phys. Rev. B **65**, 245301 (2002); A. Silva, Y. Oreg, and Y. Gefen, Phys. Rev. B **66**, 195316 (2002).
- [17] Here, as in the remainder of this paper, we consider particle currents. The displacement-current contribution has to be treated separately [9].
- [18] B. Kubala and F. Marquardt, Phys. Rev. B **81**, 115319 (2010).
- [19] A. P. Jauho, N. S. Wingreen, and Y. Meir, Phys. Rev. B **50**, 5528 (1994).
- [20] X. Q. Li and Z. B. Su, Phys. Rev. B **54**, 10807 (1996).
- [21] J. Lehmann, S. Kohler, V. May, and P. Hänggi, J. Chem. Phys. **121**, 2278 (2004).
- [22] T. A. Costi, A. C. Hewson, and V. Zlatic, J. Phys. Condens. Matter **6**, 2519 (1994).
- [23] W. Hofstetter, Phys. Rev. Lett. **85**, 1508 (2000).
- [24] A. Weichselbaum and J. von Delft, Phys. Rev. Lett. **99**, 076402 (2007).
- [25] R. Bulla, T. A. Costi, and T. Pruschke, Rev. Mod. Phys. **80**, 395 (2008).
- [26] R. Bulla, N.-H. Tong, and M. Vojta, Phys. Rev. Lett. **91**, 170601 (2003).
- [27] M. Sindel, W. Hofstetter, J. von Delft, and M. Kindermann, Phys. Rev. Lett. **94**, 196602 (2005); C. P. Moca, I. Weymann, and G. Zaránd, Phys. Rev. B **81**, 241305 (2010).
- [28] A. C. Hewson and D. Meyer, J. Phys. Condens. Matter **14**, 427 (2002).
- [29] P. S. Cornaglia, H. Ness, and D. R. Grempel, Phys. Rev. Lett. **93**, 147201 (2004); P. S. Cornaglia and D. R. Grempel, Phys. Rev. B **71**, 245326 (2005).
- [30] M. Yoshida, M. A. Whitaker, and L. N. Oliveira, Phys. Rev. B **41**, 9403 (1990); R. Zitko and T. Pruschke, Phys. Rev. B **79**, 085106 (2009).